Carrillo Abad, J.; García Gabaldón, M.; Pérez Herranz, V. (2014). Study of the zinc recovery from spent pickling baths by means of an electrochemical membrane reactor using a cation-exchange membrane under galvanostatic control. Separation and Purification Technology. 132:479-486. doi:10.1016/j.seppur.2014.05.052.

Study of the zinc recovery from spent pickling baths by means of an electrochemical membrane reactor using a cation-exchange membrane under galvanostatic control

J. Carrillo-Abad, M. García-Gabaldón* and V. Pérez-Herranz

IEC Group, Departamento de Ingeniería Química y Nuclear, Universitat Politècnica de València, Camí de Vera s/n, 46900 València, Spain. P.O. Box 22012, E-46071

*Corresponding author: Tel.: +34 963877632; Fax: +34 963867639. E-mail addresses: mongarga@iqn.upv.es (M. García-Gabaldón)

Keywords: anion-exchange membrane, cation-exchange membrane, iron codeposition, pickling solutions, zinc electrodeposition

Abstract

The performance of a cation-exchange membrane (CEM) used for recovering zinc from real spent pickling baths is studied in this work. These spent baths contain high amounts of $ZnCl_2$ and $FeCl_2$ in aqueous HCl media. The results obtained with this membrane are compared with those obtained with an anion-exchange membrane (AEM) treating the same effluent. The effect of the presence or absence of initial zinc in the cathodic compartment is also studied.

The absence of initial zinc in the cathodic compartment in the CEM experiments permits iron codeposition. Furthermore, the results obtained with the CEM are worse than those obtained with the AEM for all the figures of merit. This fact shows the need of filling the cathodic compartment with a synthetic zinc solution. The presence of zinc in the cathodic compartment from the beginning of the electrolysis not only inhibits iron deposition but also favors zinc deposition as the hydrogen evolution reaction becomes a secondary reaction, improving by this way the results of all the figures of merit of the reactor with the CEM. A deep study about the effect of the applied current and the concentration of the synthetic zinc solution placed in the cathodic compartment permits

to reach the equilibrium between the zinc transferred through the membrane and that deposited on the cathode. Therefore, the synthetic cathodic zinc is not consumed at any time. Moreover, under this circumstances iron codeposition is also avoided.

1. INTRODUCCTION

One of the most well known uses of metallic zinc is to protect iron or steel pieces from corrosion processes by coating them with it [1]. In order to coat the pieces, the oldest technique used is the hot dip galvanizing, which is based on dipping the pieces into molten zinc. Previously to the dipping process, these pieces must be cleaned by means of different pretreatments. The present paper focuses on the effluents coming from the pickling process, which consists of attacking the pieces surface with HCl for cleaning them from rust and impurities. The effluents coming from the pickling process contain high concentrations of Zn, Fe and HCl together with low concentrations of organic compounds, such as hydrogen evolution reaction inhibitors, and other heavy metals [2]. Therefore, spent pickling baths have to be treated before their disposal to accomplish with the environmental restrictions. However, the development of an adequate treatment for this effluent is very difficult because of the high complexity usually encountered in the hydrochloric acid effluents, where the target species are present in a heterogeneous mixture with different amounts of non-desirable compounds [3].

Owning to the inefficiency of the traditional methods for the treatment of spent pickling baths, as the precipitation-filtration process [4], many different techniques such as liquid-liquid extraction [5] or anionic resins [6] have been suggested [7]. In this way, the electrolysis in a membrane reactor is presented in this paper as an alternative for the treatment of the spent pickling baths in one single step. In a previous work [8], the authors performed an electrochemical study of the solution to obtain the kinetics of the electrochemical processes and, then, an undivided electrochemical batch reactor was used in potentiostatic and galvanostatic mode [9, 10] to determine the viability of zinc recovery from spent pickling baths. During these experiments zinc redissolution was observed at high time values for all the experimental conditions. This process is related to the synergic effect of iron ions and dissolved chlorine gas that attacks zinc deposits causing their oxidation [11, 12].

In order to prevent the zinc redissolution phenomena, an anion-exchange membrane (AEM) was initially used [13] to avoid chlorine presence in the cathodic compartment. This membrane permitted zinc conversion values closer to 100% and higher current efficiencies. However, iron began to codeposit with zinc as the latter was being removed from the solution since the iron-zinc system deposits following the anomalous codeposition phenomenon [14-16], in which the less noble metal (zinc) deposits preferentially, and iron deposition depends on the zinc-iron ratio, the applied current and the pH value.

Therefore, in order to recover zinc in only one step and try to prevent iron codeposition simultaneously, a cation-exchange membrane (CEM), NAFION-117, is used in the present work. In this sense, the anodic compartment contains the spent pickling bath whereas the cathodic one is filled with HCl in the presence or absence of a synthetic zinc salt. By this way, chlorine presence in cathodic compartment is avoided as CEM acts as a barrier. Moreover, the zinc pass through the cation-exchange membrane is preferential over that of iron. This is related to the Fe(II) oxidation to Fe(III) in the anodic compartment together with the fact that NAFION-117 traps trivalent cations preferentially over the divalent ones [17-19]. Therefore, the influence of the concentration of the synthetic zinc solution initially present in the cathodic compartment together with the applied current will be evaluated. In addition, the results obtained with the CEM will be compared with those obtained with the AEM at the same working conditions. For a better understanding of the different experiments, a diagram of the electrochemical reactor with both membranes used is presented in Fig. 1.

2. METHODOLOGY AND MATERIALS

The reactor used in this work was well defined in our previous work [13]. An equal volume (250 cm^3) of anolyte and catholyte is poured in their respective chamber after cell assembly. The same Ag/AgCl reference electrode and graphite cathode and anode have been used in this set-up. Both cathode and anode are totally immersed in the solution and they are symmetrically placed with respect to membrane surface. The membranes used are a NAFION-117 as CEM and an IONICS AR-204-SZRA-412 as AEM. The anode and cathode are made of two cylindrical graphite bars with an effective area of 14.15cm^2.

The average composition of the spent pickling bath used in this work is presented in Table 1. The 1:10 diluted spent pickling bath is placed in the anodic compartment and a synthetic solution composed of 0.1M HCl or 0.1M HCl and $ZnCl_2$ in a concentration range from 0.02M to 0.1M, is placed in the cathodic one for the CEM experiments. On the other hand, in the AEM experiments, the 1:10 diluted spent pickling bath is poured in the cathodic compartment whereas the anodic one is filled with a 0.1M HCl solution (Fig. 1). The synthetic solutions containing $ZnCl_2$ and/or HCl have been made from analytical grade reagents and distilled water. All experiments were made at room temperature.

Galvanostatic experiments are performed at different applied currents, which range from 700 to 1750mA. The equipment used for the electrolysis experiments is an Autolab PGSTAT20 potentiostat/galvanostat. Potential, cell voltage, current, pH and temperature are recorded during the electrowinning. On the other hand, 1ml samples are taken from the reactor every 30 minutes and zinc and iron determination is performed by atomic absorption spectrophotometry (AAS) as described in our previous works [9, 10, 13]. The determination of zinc is carried out on a Perkin–Elmer model Analyst 100 atomic absorption spectrophotometer using a zinc hollow cathode lamp at 213.9nm wavelength, 0.7nm spectral bandwidth and an operating current of 5mA, whereas iron concentration is measured using the same equipment, changing the Zn hollow lamp for a Fe hollow lamp. The parameter values used for iron determination are: a wavelength of 248.3nm, an applied operating current of 5mA and a spectral bandwidth of 0.2nm.

3- RESULTS AND DISCUSSION

As mentioned above, Nafion-117 is selected, in this work, as CEM in order to try to avoid the iron codeposition problem because this membrane favors zinc transport over that of iron. Divalent iron must be oxidized to its trivalent form in the anodic compartment and, therefore, it will be retained by Nafion-117 preferentially. With the purpose of comparing different aspects of the zinc electrodeposition, galvanostatic experiments are performed and the evolution of the concentration of zinc and iron in both the anodic and cathodic compartments is followed by means of atomic absorption

spectrometry. Various figures of merit of the electrolytic cell are calculated. Firstly, zinc and iron removal rate is calculated using Eq. (1):

$$X(t) = \frac{n_0 - n(t)}{n_0} \tag{1}$$

where n_0 are the initial mols of zinc or iron present in solution and n(t) corresponds to the mols of this species at a given time. Furthermore, the current efficiency, which is an indicative of the efficiency of the zinc deposition process and relates the current used to deposit it with the total current input, is calculated by using Eq. (2) [20]:

$$\phi(t) = \frac{n \cdot F \cdot \left(n_0 - n(t)\right)}{\int_0^t I(t)dt} \cdot 100 \quad (\%) \tag{2}$$

where n is the number of electrons exchanged in the metal deposition, F is the Faraday's constant, and I(t) is the applied current at a certain instant of time. The space-time yield is another parameter related to the achieved productivity that indicates the mass of contaminant eliminated per unit of volume and time and is defined by Eq. (3):

$$\eta(t) = \frac{M \cdot \left(n_0 - n(t)\right)}{t \cdot V} \quad (g \cdot l^{-1} \cdot h^{-1}) \tag{3}$$

where V is the reactor volume, M is the atomic weight of the species of interest and t is a given instant time. Finally, the specific energy consumption is also calculated using the following equation:

$$E_s(t) = \frac{\int_0^t U(t) \cdot I(t)dt}{M \cdot n_0 \cdot X(t)} \quad (kW \cdot h \cdot kg^{-1}) \tag{4}$$

where U(t) is the cell potential at a given instant time.

3.1. Comparison of the behavior of the CEM and the AEM

Fig. 2 shows the zinc fractional conversion (X_{Zn}) profile of the two different electrochemical reactors presented in Fig. 1 for two different values of the applied current (700 and 1000mA) when processing the 1:10 diluted spent bath. Obviously, zinc conversion values are greater for the AEM than for the CEM since the diluted spent bath is already present in the cathodic compartment from the beginning of the AEM electrolysis. On the other hand, comparing only the CEM results, an increase in the applied current produces a slight increase in the zinc conversion values obtained.

The iron conversion rate obtained for the same experimental conditions as those presented in Fig. 2 is shown in Fig. 3. It is noteworthy that iron does not deposit with zinc in a normal way but following the anomalous codeposition process [14-16]. This fact explains that iron deposits from the beginning of the electrolysis for the CEM experiments. In this case, there is not any initial zinc in the cathodic compartment, and all the zinc that comes through the membrane from the anodic compartment is immediately deposited. Since some Fe(II) also cross the membrane together with zinc, and since the zinc remaining in the cathodic compartment is very low (due to its continuous deposition as it reaches the cathodic compartment), these facts make the ratio zinc/iron be sufficiently low to allow iron codeposition practically from the initial electrolysis times. On the contrary, for the AEM assay, since zinc and iron are both initially present in the cathodic compartment, the ratio zinc/iron is maintained high enough during the first 200 minutes of electrolysis (Fig. 3) and iron deposition only starts when the zinc conversion has reached, approximately, a 60% (Fig. 4). Therefore, iron only codeposits with zinc when zinc-iron ratio becomes low. This fact is in agreement with the explanation given by *Dahms et al.* [21] about the anomalous codeposition process, which is based on the formation of a zinc hydroxide film on the cathode surface that inhibits iron deposition. However, as zinc is being depleted from solution this film becomes weaker and iron begins to codeposit with zinc. In the CEM experiments it can also be observed that the higher the applied current, the higher the iron fractional conversion.

The bulk solution pH in the cathodic compartment has been measured over all the experiment time as can also be observed in Fig. 3. For all the cases under study, the pH

in the cathodic compartment increases with time due to the protons consumption related to hydrogen evolution reaction. A pH increase is always observed when iron begins to codeposit with zinc. This fact may be associated with the pH effect on the iron deposition observed in our previous works [8], where the inhibition of iron deposition at low pH solutions was observed. In the case of the AEM experiments, when the pH parameter reaches a value close to 2, the iron conversion starts. On the other hand, in the case of the CEM, since the pH value is higher or equal to 2 during practically all the electrolysis time, the iron codeposits with zinc from the beginning of the electrolysis

The evolution with time of the zinc current efficiency (ϕ) for the same experimental conditions as those presented above is shown in Fig. 5. In this figure, the CEM results present the lowest values of ϕ. These results are related to the fact that at the first stages of the electrolysis, hydrogen evolution reaction is the main reaction as zinc has to pass through the membrane prior to be deposited and, in addition, iron codeposits with zinc from the beginning of the electrolysis. As shown in Fig. 5, the higher the applied current the lower the current efficiency is, as expected by the results obtained in previous works [10, 13]. In the case of the experiment performed in the presence of the AEM zinc does not have to pass through the membrane before being deposited and, thus, zinc is the main reaction whereas HER process becomes a parallel reaction. Therefore, the zinc current efficiency value in the presence of the AEM is higher than that obtained in the case of the CEM.

The evolution with time of the zinc space-time-yield (η) is shown in Fig. 6 for the experimental conditions explained previously. In all cases, zinc space-time yield increases at the first electrolysis stages due to zinc nucleation on the cathode surface which causes a decrease in the electrode resistance and favors zinc deposition, and then η decreases due to zinc depletion from solution. However, the highest η values are obtained using the AEM since all the zinc is placed in the cathodic compartment from the beginning of the electrolysis. In the experiments in the presence of the CEM, as zinc must be transported through the membrane before its deposition, its nucleation on the graphite electrode is slower and this fact results in the lower values of η observed in Fig. 6. On the other hand, an increase in the applied current results in a higher rate of zinc deposition, and consequently, η increases as well.

Fig. 7 presents the results obtained for the zinc specific energy consumption (E_S) for the cases studied above. In the presence of the CEM, the energy consumed for zinc deposition presents the highest values and increases with time and with the applied current value, as expected [10, 13]. The highest E_S values are obtained for the CEM since HER process is the main reaction at the first electrolysis stages and iron deposition takes place from the beginning consuming a large amount of energy. In addition, another process that consumes energy in the CEM experiments is the transport of the ions through the membrane from the anodic chamber to the cathodic one. On the other hand, AEM presents the lowest values as zinc is present in the cathodic compartment from the beginning of the electrolysis.

3.2. Effect of zinc presence in the cathodic compartment of the reactor

Summarizing the previous results obtained for both membrane reactors, the reactor with the AEM provides better results for all the figures of merit. These worse results obtained for the reactor in the presence of the CEM are related to the zinc absence in the cathodic compartment during the initial instants of the electrolysis that causes the setting up of HER as the main reaction during these initial moments. In addition, this absence of zinc in the cathodic chamber gives rise to the decrease of the zinc/iron ratio up to the point that the zinc hydroxide film becomes sufficiently weak to permit iron codeposition. In order to solve these problems related to the zinc absence, the cathodic compartment is initially filled with a solution composed of 0.1M $ZnCl_2$ in 0.1M HCl, and the effect of this cathodic zinc presence on the different figures of merit as well as on the iron codeposition is evaluated at different applied currents.

Fig. 8 a) represents the evolution of the total mols of zinc deposited (Zn_d) for both the AEM and the CEM with (Zn_C0≠0) and without (Zn_C0=0) initial zinc present in the cathodic compartment. This Figure presents moles of zinc deposited rather than rate of zinc conversion because the total initial concentration of zinc is different when adding zinc in the cathodic compartment, and under these circumstances the conversion in terms of X is not convenient. As can be seen in this figure, adding initial zinc in the cathodic compartment improves the electrochemical reactor performance up to the point that the values obtained in the CEM ZnC0≠0 experiment equalize to those obtained in the AEM assays. This is based on the fact that both experiments present the same value

of applied current (1A) and there is zinc from the beginning of the electrolysis near the cathode permitting, by this way, its deposition.

The iron conversion results and the zinc-iron ratio evolution are shown in Fig. 8 b) and c), respectively. The presence of zinc from the beginning of the electrolysis in the CEM reactor prevents iron codeposition, which provides a method to obtain zinc and iron separately. This is associated with the fact that, when zinc is present from the initial instants of the electrolysis in the cathodic compartment, the zinc-iron ratio is maintained sufficiently high during all the experiment and no iron deposition is permitted. Therefore, the use of the CEM with this initial zinc placed in the cathodic compartment shows an advantage with regard to the behavior of the reactor with the AEM since, as mentioned above, iron codeposits with zinc in the AEM assays when zinc conversion reaches, approximately, a 60%, and the zinc-iron ratio decreases to values lower than 0.6. In addition, when no initial zinc is added, iron codeposits with zinc from the beginning of the experiment since iron is transported through the membrane together with zinc and, therefore, the zinc-iron ratio could diminish up to the point that the zinc hydroxide film becomes weaker permitting iron codeposition. This fact is in accordance with the data presented in Fig. 8 c) for the CEM Zn_C0=0 experiment, where the zinc-iron ratio remains lower than 0.6 during all of the electrolysis. In this sense, when zinc is initially present in the cathodic compartment (CEM Zn_C0≠0 experiment) no iron deposition has been observed since the presence of this zinc in the cathodic compartment maintains the zinc-iron ratio sufficiently high to prevent iron codeposition since, as shown in Fig. 8 c), the zinc-iron ratio is higher than 0.6 for all time values. Therefore, a relationship may be suggested between the zinc-iron ratio and the iron codeposition phenomenon: iron codeposition begins when zinc-iron ratio diminishes below 0.6 [22].

The bulk cathodic pH evolution with time has also been studied for the same experimental conditions as those presented previously (not shown). Once more, for all the cases under study, the pH increases with time as a consequence of the hydrogen evolution reaction. The conclusions are similar to those mentioned previously in Fig. 3, in the presence of the AEM: when a higher increase of the pH value is detected, which reaches a value close to 2, the iron codeposition begins. In the case of the CEM Zn_C0=0 experiment, the pH value is higher than 2 during practically all the

electrolysis time and, consequently, iron codeposits with zinc from the beginning of the electrolysis. On the other hand, for the CEM Zn_C0≠0 experiment, iron codeposition is not detected which is in accordance with the pH data lower than 2 for all the electrolysis time.

Figs. 8 d) to f) show the rest of the figures of merit analyzed previously (ϕ, η and E_s) for the AEM and the CEM with (Zn_C0≠0) and without (Zn_C0=0) initial zinc present in the cathodic compartment. Regarding zinc current efficiency, Fig. 8 d), the experiments in the presence of the AEM and the CEM with initial zinc in the cathodic chamber (ZnC0≠0) reach similar values. This is related to the fact that thanks to the zinc presence from the beginning of the electrolysis in the cathodic compartment, the hydrogen evolution reaction (HER) becomes a secondary reaction as in the case of the AEM experiment, and the total amount of zinc deposited is very similar in both experiments (Fig. 8 a)). In addition, the prevention of iron codeposition process in the CEM ZnC0≠0 experiment makes its zinc current efficiency be slightly higher than that in the presence of the AEM for intermediate time values.

Zinc space-time yield is compared for both reactors and for both initial conditions in Fig. 8 e). Adding initial zinc in the cathodic compartment in the CEM electrolysis increases the zinc space-time values as zinc deposition is the main reaction from the first electrolysis stages. Therefore, the values obtained for the CEM with initial zinc in the cathodic compartment, and for the AEM are very similar as the applied current is the same and the total amount of deposited zinc is also similar (Fig. 8 a)). Comparing the CEM experiments, the experiment with initial cathodic zinc (CEM Zn_C0≠0 experiment) presents higher space-time yield as the presence of zinc in the cathodic compartment from the beginning of the electrolysis permits a higher zinc deposition rate.

Fig. 8 f) presents the results obtained for the zinc specific energy consumption for the cases studied above. When zinc is added in the cathodic compartment in the presence of the CEM, E_S values are close to those obtained with the AEM because iron deposition is inhibited by the zinc presence and only the HER process competes with zinc deposition. For both CEM ZnC0≠0 and AEM experiments, the calculated E_S values are lower than those obtained in the CEM ZnC0=0 experiment since, in the first two cases, zinc is

present from the beginning of the electrolysis near the cathode. Moreover, since in this latter experiment, iron codeposition is present from the initial moments of the electrolysis, higher amounts of energy are consumed, which is reflected by the continue increase of the E_S value observed in Fig. 8 f), since iron deposition has an additional energetic cost.

Once the benefits of adding an initial amount of zinc in the cathodic compartment have been confirmed for the CEM reactor, an analysis of the effect of the applied current in these conditions is presented. In addition, in order to study the behavior of the CEM reactor with initial zinc in the cathodic compartment, it is necessary to compare the total amount of zinc deposited on the cathode (Zn_d) with the zinc that passes through the membrane from the anodic chamber (Zn_p). The objective of this comparison is to reach and equilibrium between Zn_d and Zn_p, which would mean that the synthetic zinc added in the cathodic compartment to avoid iron codeposition, is not consumed at any time.

The evolution of the amount of zinc transported through the CEM and the total zinc deposited on the graphite electrode when the applied current ranges from 700 to 1500mA is shown in Fig. 9 a) and b), respectively. Both zinc amounts, Zn_d and Zn_p, increase with the applied current, as expected. However, the amount of zinc transported through the membrane is, for all the applied currents under study, lower than the amount of zinc deposited on the cathode. This fact means that the synthetic zinc added to the cathodic compartment will be consumed at long experiment times, and the higher the applied current the lower the time needed for the depletion of the initial cathodic zinc. In addition, these figures also help to explain the fact that iron codeposits from the beginning of the experiment when no initial zinc is added to the cathodic compartment (Figs. 3 and 8 b)). Since the zinc deposition rate is higher than the zinc transport rate through the cation-exchange membrane, then zinc concentration in the cathodic compartment becomes too low to maintain the zinc-iron ratio high enough to keep the hydroxide film on the cathode surface.

The same comparison for iron is carried out in Figs. 10 a) and b). In this case, the iron transported through the membrane (Fe_p) is greater than the iron deposited (Fe_d) on the cathode surface for all the applied currents. In addition, iron deposition is observed

for applied current values higher than 1000mA as zinc is being removed from solution. If Figs. 10 a) and 9 a) are compared, it is inferred that the iron transport rate through the membrane is lower than that obtained for zinc. Moreover, this difference between both transport rates increase with time, as iron is oxidized in the anodic compartment. This fact is in agreement with the NAFION-117 capacity of trapping trivalent ions.

The previous results presented in Figs. 9 and 10, suggest that the optimum equilibrium conditions are not reached for the applied currents tested as the zinc deposited on the cathode is always higher than the zinc that goes through membrane, and consequently, the added cathodic zinc is always consumed. This situation could be avoided by modifying different parameters: one possible solution would be to increase the applied current in order to enhance the rate of zinc that passes through the membrane, and on the other hand, another possible solution would be to reduce the concentration of the zinc added to the cathodic compartment in an attempt to diminish the rate of zinc deposited on the cathode surface.

Previously to the increase of the applied current, the limiting current value of the CEM (I_{lim}) was calculated from the polarization curves of the membrane [23] (not shown). A polarization curve reflects the relationship between the current through a membrane and the corresponding voltage drop over that membrane and the adjacent boundary layers. The determination of I_{lim} provides information about ion transport limitation in ion-exchange membrane systems [24]. Under the experimental conditions presented in this work, the calculated I_{lim} value was set at 1690mA. Then, an applied current of 1750mA was selected in order to follow the study presented in Fig. 9. When this experiment finished, the appearance of a Fe(III) precipitate located at the anodic solution–membrane interface was evident. The presence of this precipitate even at high HCl concentrations is the consequence of the water splitting phenomenon that takes place under overlimiting current conditions. In this case, the protons, produced as a consequence of water splitting, are transferred through the CEM from the anodic compartment and are responsible for the pH increase in the vicinity of the membrane-solution interface, and the consequent, metal precipitation. Increasing the membrane area would allow to apply higher applied currents before the hydroxide precipitation takes place, however, this would require another experimental set-up, therefore, the decrease of the cathodic zinc concentration has been considered as the last option in

order to try to achieve the required equilibrium conditions mentioned above. In this context, two different concentration values of the cathodic zinc were tested: 0.02M and 0.05M.

The evolution of the total zinc and iron deposited on the graphite electrode and the amount of zinc and iron transported through the CEM for an applied current of 1A and when the solution placed in the cathodic compartment is composed of 0.02M $ZnCl_2$ and 0.1M HCl is shown in Fig. 11. In this case, the amount of zinc transported through the membrane is practically the same as the zinc deposited on the cathode. This fact means that the zinc present in the solution of the cathodic compartment (0.02M $ZnCl_2$ and 0.1M HCl) is not consumed at any time. However, part of the Fe(II) that crosses the membrane is later deposited in the cathodic compartment.

Fig 12 shows the same type of graphics as that presented in Figs. 11 when the solution placed in the cathodic compartment is composed of 0.05M $ZnCl_2$ and 0.1M HCl. In this case, the amount of zinc transported through the membrane is also practically the same as the zinc deposited on the cathode. On the other hand, the moles of deposited iron are considered to be negligible.

Summarizing the results presented in this point, it is inferred that the only way to avoid iron codeposition in the presence of the CEM is by adding a synthetic zinc solution in the cathodic compartment so as to keep the ratio Zn/Fe high enough. However, if this synthetic solution is very concentrated in zinc, as in the case of the solution composed of 0.1M $ZnCl_2$ and 0.1M HCl, then, the synthetic zinc added will be inevitably consumed, and this fact will also lead to the iron codeposition at some point of the electrolysis. This fact is enhanced at high time values and high applied currents. A synthetic solution composed of 0.05M $ZnCl_2$ and 0.1M HCl is found to be the optimum since allows zinc deposition avoiding practically iron codeposition, and the consumption of the synthetic zinc added to the catholyte is negligible.

4- CONCLUSIONS

A cation-exchange membrane (CEM) was employed in an electrochemical reactor under galvanostatic mode in order to recover zinc from the 1:10 diluted spent pickling baths

coming from the hot dip galvanizing industry. This membrane provided worse results than an anion-exchange membrane (AEM) in terms of figures of merit when the zinc was absent in the cathodic compartment since the zinc must pass through the membrane before being deposited. Moreover, iron codeposition was present for both types of membranes.

In the case of the CEM, the zinc presence from the beginning of the electrolysis in the cathodic compartment for a concentration value of 0.1M, improved all the figures of merit as this initial zinc presence not only inhibited iron deposition but also made hydrogen evolution reaction become a secondary reaction. However, under these experimental conditions, the zinc transport rate through the membrane was lower than its deposition rate for all the applied currents under study. With regard to iron behavior, its transport and deposition rates also increased with the applied current. It is worth to note that iron deposition was observed for applied currents higher than 1250mA as for lower current values, the zinc hydroxide film was maintained during all the electrolysis. However, for all the applied currents under study, its transport rate became lower than that of zinc as iron was being oxidized at the anodic compartment.

Different experimental parameters such as the applied current or the cathodic zinc concentration were modified in an attempt to reach the equilibrium conditions between the zinc transported through the membrane and the zinc deposited on the cathode surface. An increase of the applied current led to the formation of an iron precipitate on the anodic side of the CEM as the limiting current was surpassed. On the other hand, the decrease of the cathodic zinc concentration from 0.1M to 0.05M resulted to be the best option as not only permitted to reach the equilibrium between the zinc transferred through the membrane and that deposited on the cathode, but also iron codeposition was also avoided under this circumstances.

ACKNOWLEDGEMENTS

The authors want to express their gratitude to the Generalitat Valenciana for a postgraduate grant (GV/2010/029) and to the Ministerio de Economía y Competitividad for financing the project number CTQ2012-37450-C02-01/PPQ.

REFERENCES

[1] A. R. Marder, The metallurgy of zinc-coated steel, Prog. Mater. Sci. 45 (2000) 191-271.

[2] U. Kerney, Treatment of spent pickling acids from hot dip galvanizing, Resour. Conserv. Recy. 10 (1994) 145–151.

[3] J. A. Carrera, E. Bringas, M.F.S. Roman, I. Ortiz, Selective membrane alternative to the recovery of zinc from hot-dip galvanizing effluents, J. Membr. Sci. 326 (2009) 672–680.

[4] G. Csicsovszki, T. Kékesi, T.I. Török, Selective recovery of Zn and Fe from spent pickling solutions by the combination of anion exchange and membrane electrowinning techniques, Hydrometallurgy 77 (2005) 19–28.

[5] M. Regel-Rosocka, M. Wisniewski, Selective removal of Zn(II) from spent pickling solutions in the presence of iron ions with phosphonium ionic liquid Cyphos IL 101, Hydrometallurgy 110 (2011) 85-90.

[6] E. Marañón, Y. Fernández, F. J. Suárez, F. J. Alonso, H. Sastre, Treatment of acid pickling baths by means of anionic resins, Ind. Eng. Chem. Res. 39 (2000) 3370-3376.

[7] M. Regel-Rosocka, A review on methods of regeneration of spent pickling solutions from steel processing, J. Hazard. Mater. 177 (2010) 57-69.

[8] M. García-Gabaldón, J. Carrillo-Abad, V. Pérez-Herranz, E. M. Ortega-Navarro, Electrochemical study of a simulated spent pickling solution, Int. J. Electrochem. Sci. 6 (2011) 506–519.

[9] J. Carrillo- Abad, M. García-Gabaldón, E. Ortega, V. Pérez-Herranz, Electrochemical recovery of zinc from the spent pickling baths coming from the hot dip galvanizing industry. Potentiostatic operation, Sep. Purif. Technol. 81 (2011) 200–207.

[10] J. Carrillo-Abad, M. García-Gabaldón, V. Pérez-Herranz, Electrochemical recovery of zinc from the spent pickling solutions coming from hot dip galvanizing industries. Galvanostatic operation, Int. J. Electrochem. Sci. 7 (2012) 5442–5456.

[11] O. Caldwell-Ralston, Electrolytic Deposition and Hydrometallurgy of Zinc, McGraw-Hill Book Company Inc., New York, 1921.

[12] B.K. Thomas, D.J. Fray, The effect of additives on the morphology of zinc electrodeposited from a zinc chloride electrolyte at high current densities, J. Appl. Electrochem. 11 (1981) 677–683.

[13] J. Carrillo-Abad, M. García-Gabaldón, E. Ortega, V. Pérez-Herranz, Recovery of zinc from spent pickling solutions using an electrochemical reactor in

presence and absence of an anion-exchange membrane: Galvanostatic operation, Sep. Purif. Technol. 98 (2012) 366-374.

[14] P. Díaz-Arista, O.R. Mattos, O.E. Barcia, F.J. Fabri Miranda, ZnFe anomalous electrodeposition: stationaries and local pH measurements, Electrochim. Acta 47 (2002) 4091–4100.

[15] E. Gómez, E. Peláez, E. Vallés, Electrodeposition of zinc + iron alloys: I. Analysis of the initial stages of the anomalous codeposition, J. Electroanal. Chem. 469 (1999) 139–149.

[16] Z. Zhang, W.H. Leng, H.B. Shao, J.Q. Zhang, J.M. Wang, C.N. Cao, Study on the behavior of Zn–Fe alloy electroplating, J. Electroanal. Chem. 516 (2001) 127–130.

[17] R.F. Dalla Costa, J.Z. Ferreira, C. Deslouis, Electrochemical study of the interactions between trivalent chromium ions and Nafion-117 perfluorosulfonated membranes, J. Membr. Sci. 215 (2003) 115–128.

[18] T. Okada, Y. Ayato, M. Yuasa, I. Sekine, The effect of impurity cations on the transport characteristics of perfluorosulfonated ionomer membranes, J. Phys. Chem. 103 (1999) 3315–3322.

[19] M. Taky, G. Pourcelly, C. Gavach, A. Elmidaoui, Chronopotentiometric response of a cation exchange membrane in contact with chromium(III) solutions, Desalination 105 (1996) 219–228.

[20] S. Koter, A. Narebska, Current efficiency and transport phenomena in systems with charged membranes, Sep. Sci. Technol. 24 (1989) 1337-1354.

[21] H. Dahms, I. M. Croll, The anomalous codeposition of iron-nickel alloys, J. Electrochem. Soc. 112 (1965) 771-775.

[22] J. Carrillo-Abad, M. García-Gabaldón, V. Pérez-Herranz. Treatment of spent pickling baths coming from hot dip galvanizing by means of an electrochemical membrane reactor, Desalination (2013), http://dx.doi.org/ 10.1016/j.desal.2013.11.040

[23] M. C. Martí-Calatayud, M. García-Gabaldón, V. Pérez-Herranz, E. Ortega, Determination of transport properties of Ni(II) through a Nafion cation-exchange membrane in chromic acid solutions, J. Membr. Sci. 379 (2011) 449-458.

[24] P. Długołęcki, B. Anet, S. J. Metz, K. Nijmeijer, M. Wessling, Transport limitations in ion exchange membranes at low salt concentrations, J. Membr. Sci. 346 (2010) 163-171.

Figures and Tables

Table 1. Average composition, in mol/l and g/l, of the spent pickling bath used in this work

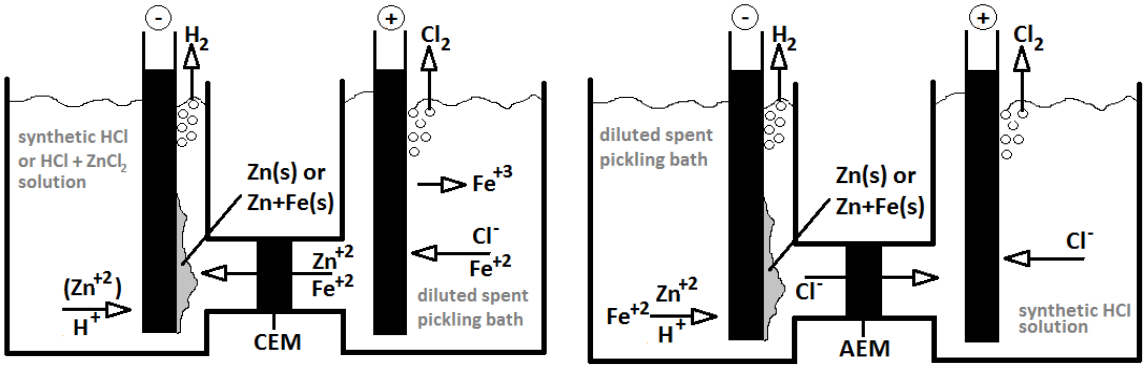
-
H2
+
Cl2
synthetic HCl
or HCl + ZnCl2
solution
Zn(s) or
Zn+Fe(s)
Fe+3
Cl-
Fe+2
Zn+2
Fe+2
(Zn+2)
H+
diluted spent
pickling bath
CEM
-
H2
+
Cl2
diluted spent
pickling bath
Zn(s) or
Zn+Fe(s)
Cl-
Zn+2
Fe+2
H+
Cl-
synthetic HCl
solution
AEM

Figure 1

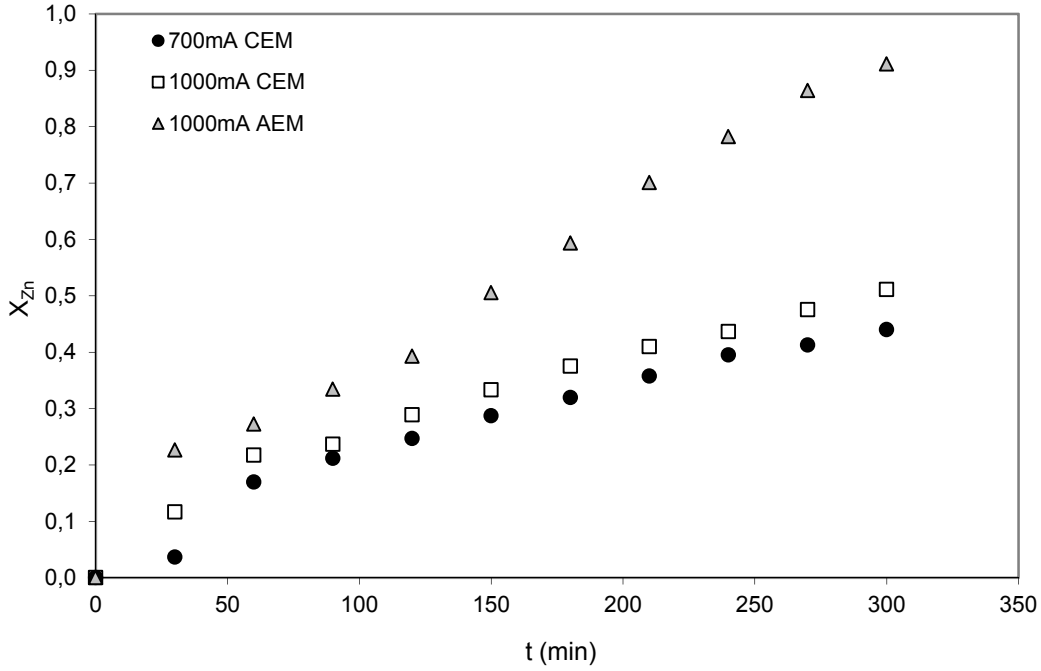
700mA CEM
1000mA CEM
1000mA AEM
X_{Zn}
t (min)
0,0
0,1
0,2
0,3
0,4
0,5
0,6
0,7
0,8
0,9
1,0
0
50
100
150
200
250
300
350

Figure 2

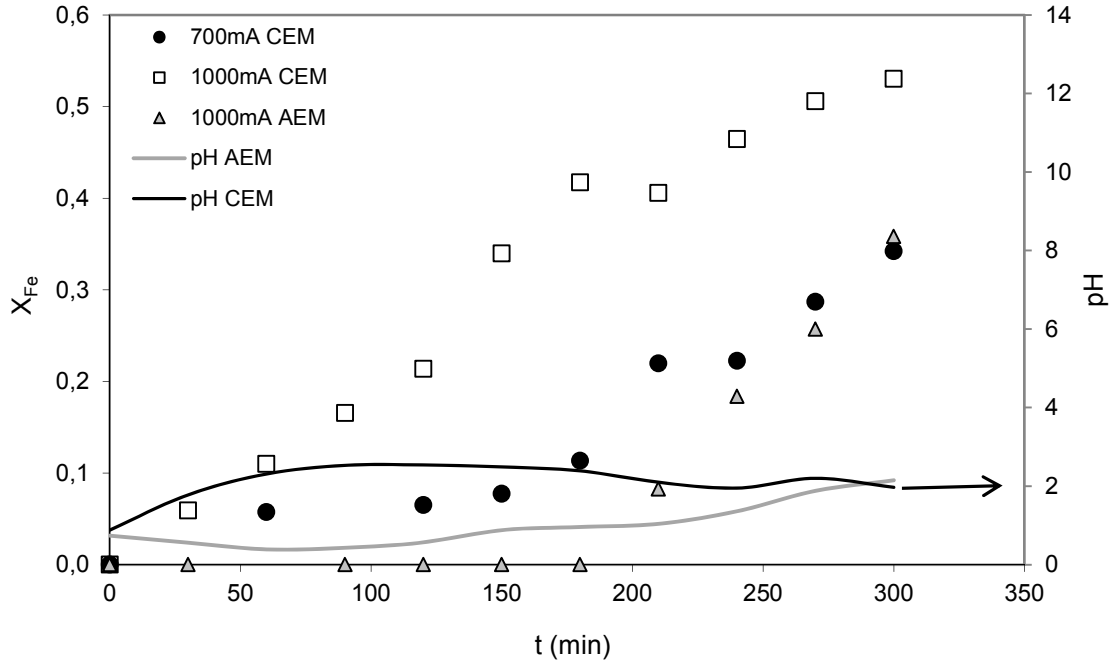
0,6
0,5
0,4
0,3
0,2
0,1
0,0
X_{Fe}
14
12
10
8
6
4
2
0
pH
0
50
100
150
200
250
300
350
t (min)
700mA CEM
1000mA CEM
1000mA AEM
pH AEM
pH CEM

Figure 3

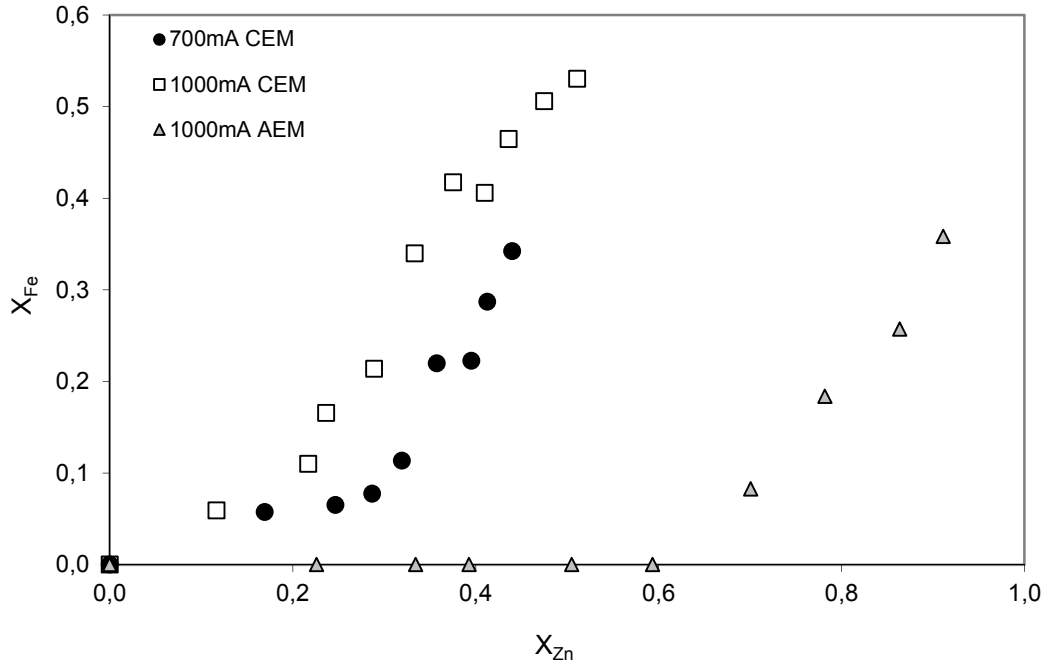
0,6
0,5
0,4
0,3
0,2
0,1
0,0
X_{Fe}
700mA CEM
1000mA CEM
1000mA AEM
0,0
0,2
0,4
0,6
0,8
1,0
X_{Zn}

Figure 4

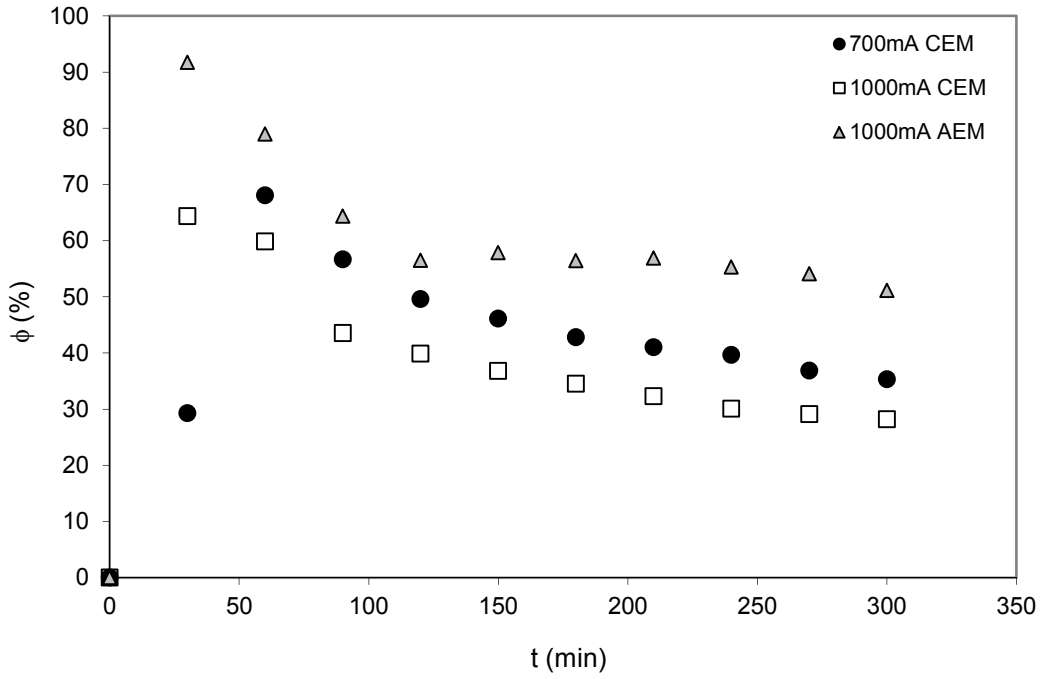
100
90
80
70
60
50
40
30
20
10
0
ϕ (%)
0
50
100
150
200
250
300
350
t (min)
700mA CEM
1000mA CEM
1000mA AEM

Figure 5

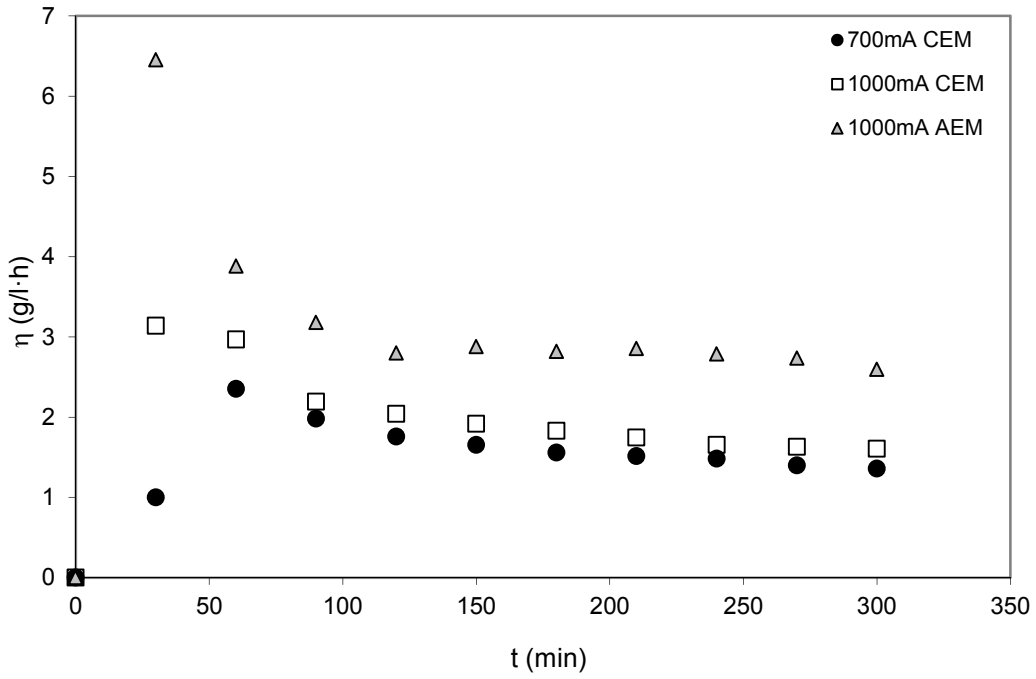
700mA CEM
1000mA CEM
1000mA AEM
η (g/l·h)
t (min)
0
1
2
3
4
5
6
7
0
50
100
150
200
250
300
350

Figure 6

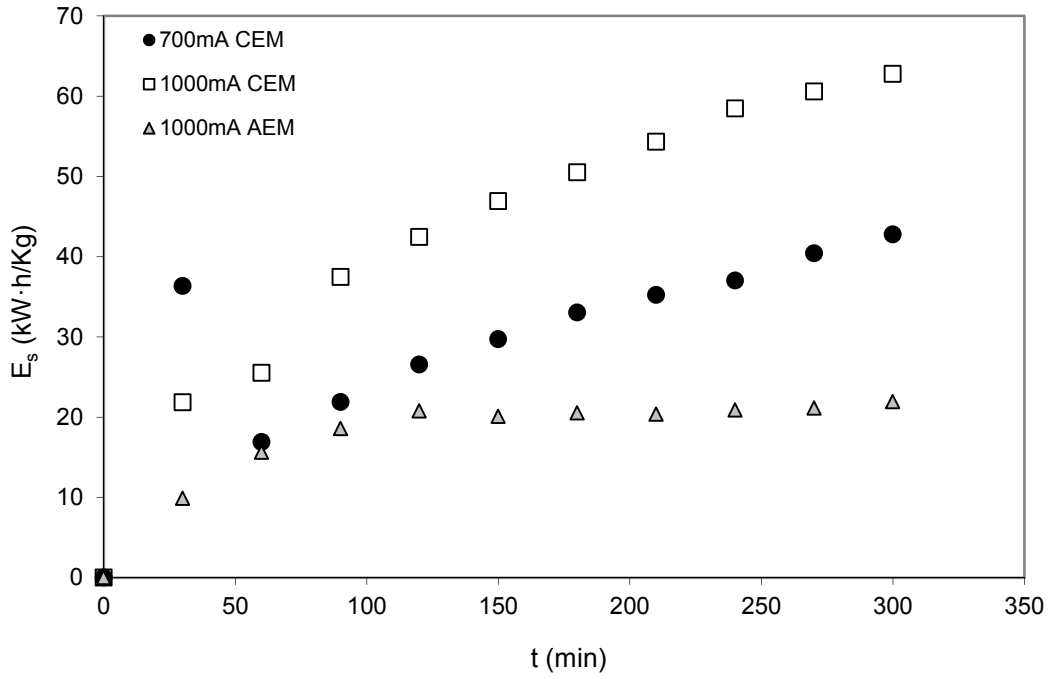
700mA CEM
1000mA CEM
1000mA AEM
E_s (kW·h/Kg)
t (min)
0
10
20
30
40
50
60
70
0
50
100
150
200
250
300
350

Figure 7

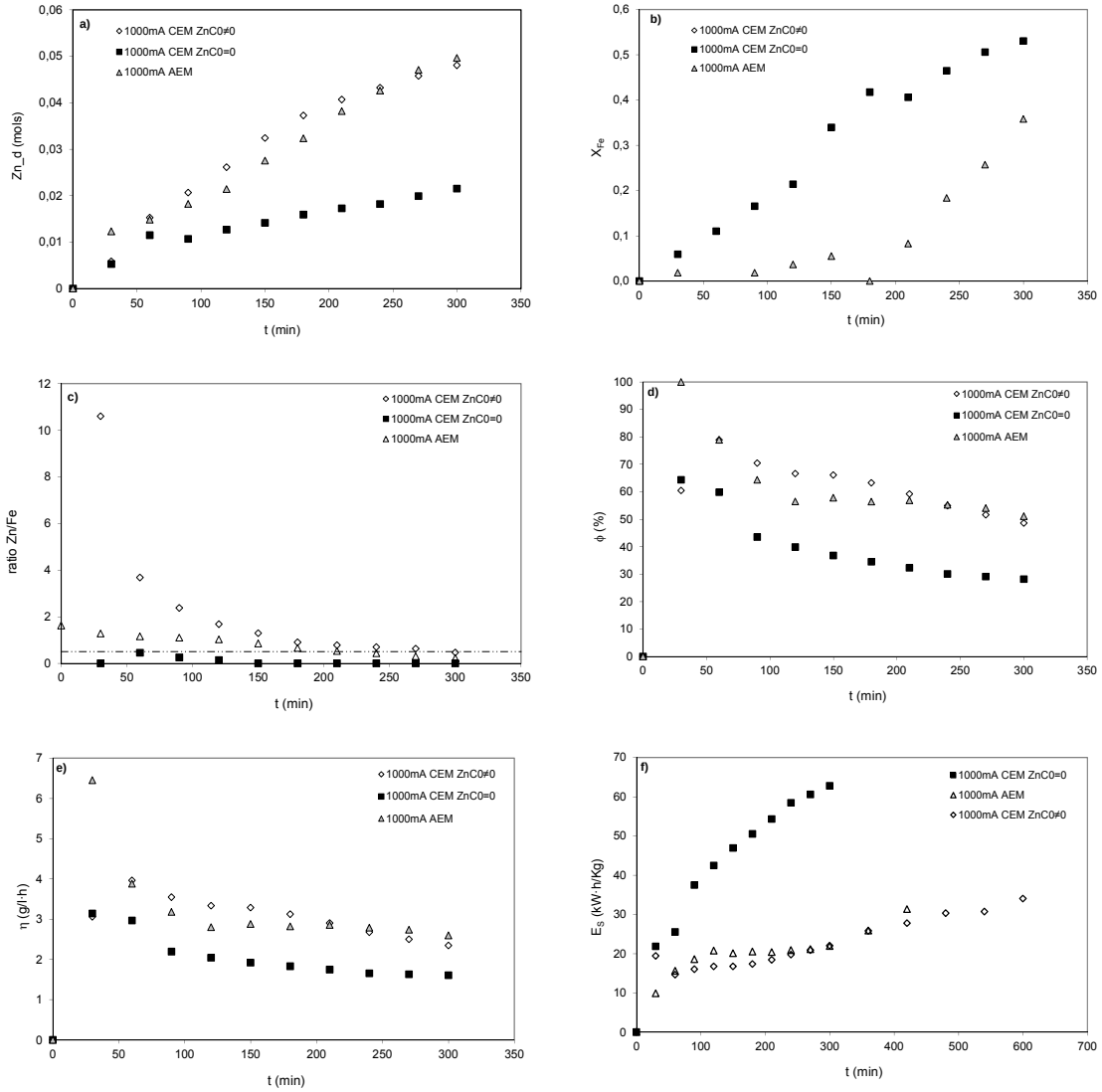
a)
1000mA CEM ZnC0≠0
1000mA CEM ZnC0=0
1000mA AEM
Zn_d (mols)
t (min)
b)
X_{Fe}
c)
ratio Zn/Fe
d)
ϕ (%)
e)
η (g/l·h)
f)
E_S (kW·h/Kg)

Figure 8

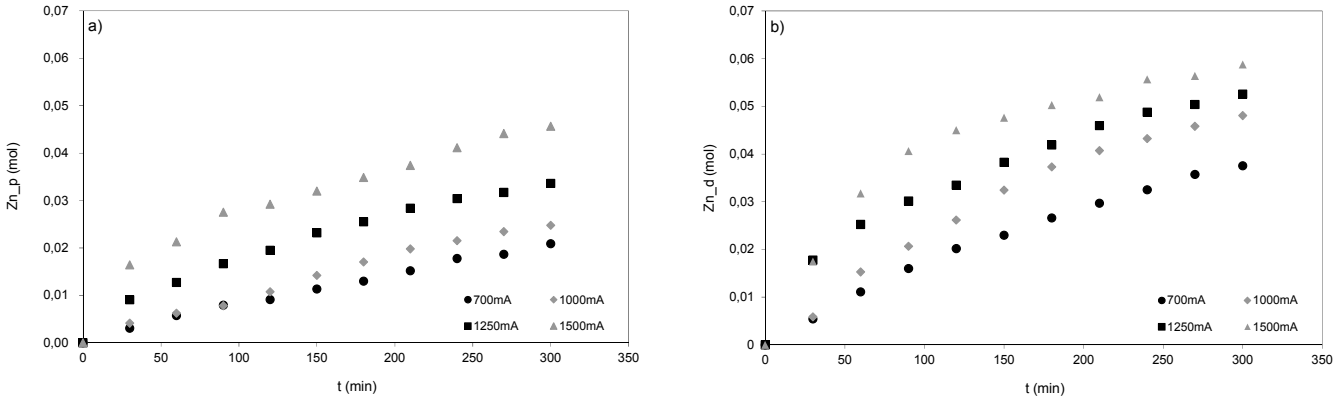
a)
Zn_p (mol)
0,07
0,06
0,05
0,04
0,03
0,02
0,01
0,00
0
50
100
150
200
250
300
350
t (min)
700mA
1000mA
1250mA
1500mA
b)
Zn_d (mol)
0,07
0,06
0,05
0,04
0,03
0,02
0,01
0
0
50
100
150
200
250
300
350
t (min)
700mA
1000mA
1250mA
1500mA

Figure 9

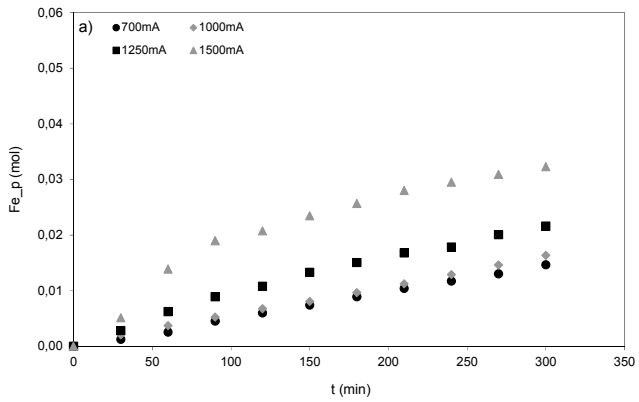
a)
700mA
1000mA
1250mA
1500mA
Fe_p (mol)
t (min)
0,00
0,01
0,02
0,03
0,04
0,05
0,06
0
50
100
150
200
250
300
350

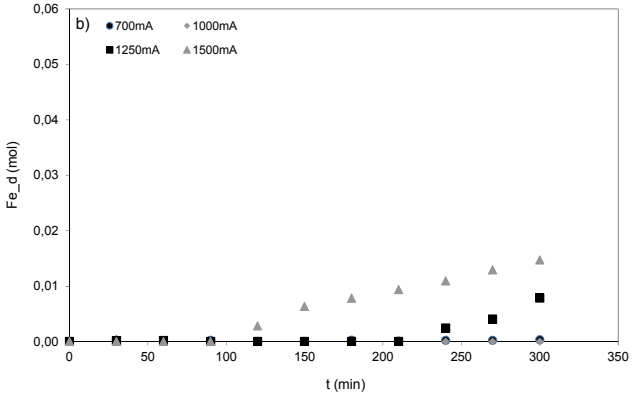
b)
700mA
1000mA
1250mA
1500mA
Fe_d (mol)
t (min)
0,00
0,01
0,02
0,03
0,04
0,05
0,06
0
50
100
150
200
250
300
350

Figure 10

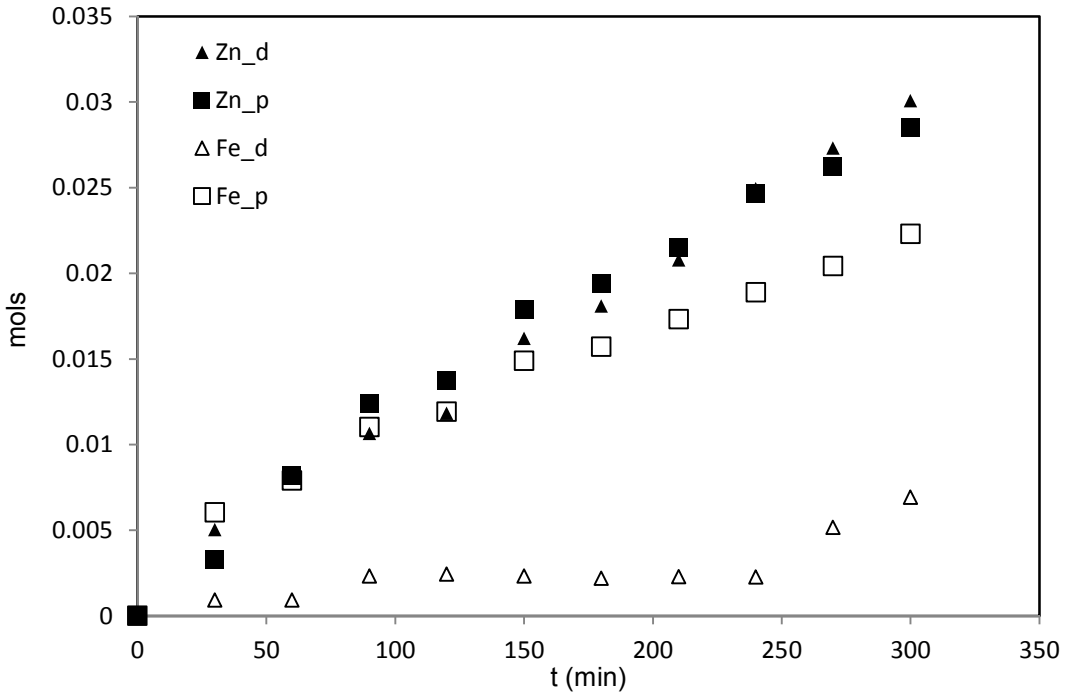
0.035
0.03
0.025
0.02
0.015
0.01
0.005
0
mols
Zn_d
Zn_p
Fe_d
Fe_p
0
50
100
150
200
250
300
350
t (min)

Figure 11

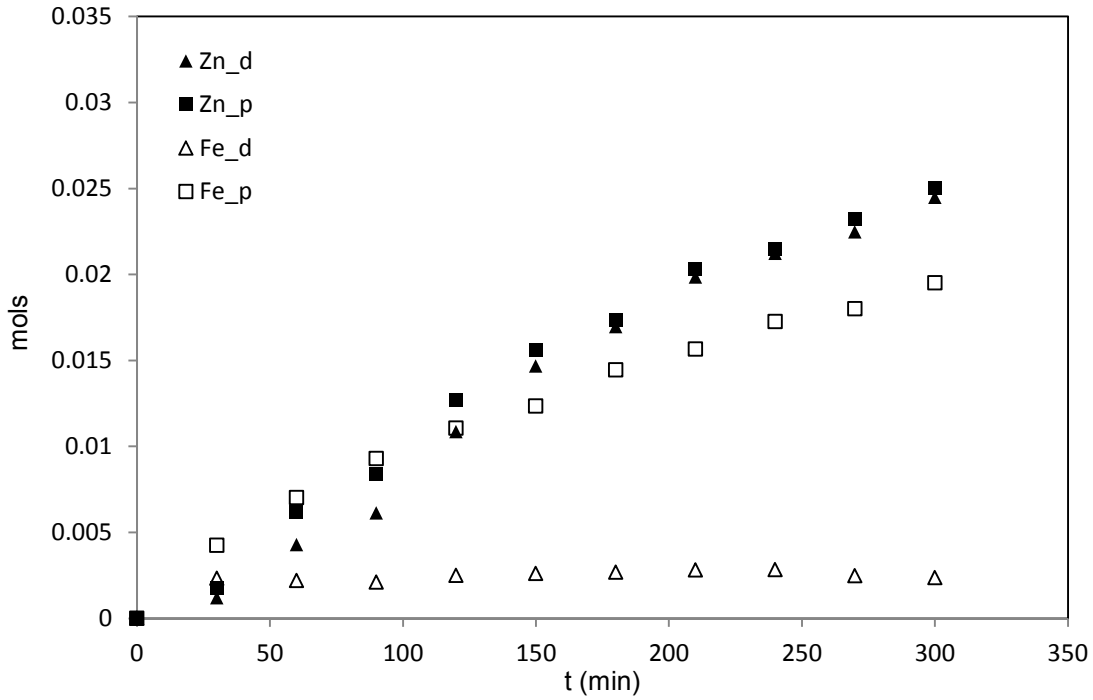
0.035
0.03
0.025
0.02
0.015
0.01
0.005
0
mols
Zn_d
Zn_p
Fe_d
Fe_p
0
50
100
150
200
250
300
350
t (min)

Figure 12

Table 1

Average composition, in mol/l and g/l, of the spent pickling bath used in this work

	Zn	**Fe**	**HCl**
M	1.9780	1.0578	2.1380
g/l	129.3242	58.8129	78.0356